

ARGO: a model for accurate estimation of influenza epidemics using Google search data

Shihao Yang^{*1}, Mauricio Santillana^{†2,3}, and S. C. Kou^{‡1}

¹Department of Statistics, Harvard University, Cambridge, MA, USA

²School of Engineering and Applied Sciences, Harvard University, Cambridge, MA, USA

³Boston Children’s Hospital Informatics Program, Boston, MA, USA

April 26, 2022

Abstract

Accurate real-time tracking of influenza outbreaks helps public health officials make timely and meaningful decisions that could save lives. We propose a new influenza tracking model, ARGO (AutoRegression with GOogle search data), that uses publicly available online search data. In addition to having a rigorous statistical foundation, ARGO outperforms all previously available tracking models, including the latest version of Google Flu Trends (GFT), even though it uses only low-quality search data as input from publicly available *Google Trends* and *Google Correlate* websites. ARGO not only incorporates the seasonality in influenza epidemics, but also captures changes in people’s online search behavior over time. ARGO is also flexible, self-correcting, robust and scalable, making it a potentially powerful tool that can be used for real-time tracking of other social events at multiple temporal and spatial resolutions.

Keywords — Digital disease detection, Google Flu Trends, Seasonal Influenza, Big Data, Real-time estimation of influenza-like illnesses activity, Autoregressive-exogenous model, L_1 regularization

Big data sets are constantly generated nowadays as the activity patterns of millions of users are collected from internet-based services. Numerous studies have proposed early prototypes, showing great potential of these big data sets to detect and manage epidemic outbreaks (Influenza [1, 2, 3, 4, 5, 6], Ebola [7], Dengue [8]), predict changes in stock prices [9, 10] and housing prices [11], estimate users’ movie preferences [12], etc. In 2009, Google Flu Trends (GFT), a digital disease detection system that uses the volume of selected Google search terms to estimate current influenza-like illnesses (ILI) activity, was identified by many as a good example of how *big data* would transform traditional statistical predictive analysis [13].

However, a collection of significant discrepancies between GFT’s flu estimates and those measured by the Centers for Disease Control led to considerable doubt regarding the value of digital disease detection systems in subsequent years [14]. While multiple revisions have identified methodological flaws in GFT’s original algorithm [15, 16, 17] and have led to incremental improvements [15, 17, 18, 19], a statistical framework that is theoretically sound and capable of generating accurate estimations is still lacking. Here we present such a framework that culminates in a new method which outperforms all existing methodologies for tracking influenza activity.

*shihaoyang@g.harvard.edu

†msantill@fas.harvard.edu

‡kou@stat.harvard.edu; corresponding author

Influenza outbreaks cause up to 500,000 deaths a year worldwide, and an estimated 3,000 to 50,000 deaths a year in the United States of America [20]. Our ability to effectively prepare for and respond to these outbreaks relies heavily on the availability of accurate estimation of their activities in real time. Existing methods to predict the timing, duration, and magnitude of influenza outbreaks remain limited [21]. Well-established clinical methods to track flu activity, such as the Centers for Disease Control’s (CDC) ILINet, typically report information with a lag of 1-3 weeks (<http://www.cdc.gov/flu/>). This time lag is far from optimal for decision-making purposes.

In order to alleviate this information gap, multiple methodologies combining climate data, demographic data, and epidemiological data with mathematical models have been proposed to infer real-time estimates and forecasts of flu activity [21, 22, 23, 24, 25, 26]. In recent years, non-traditional methodologies have also been proposed in order to harness internet-based information such as: Google [1], Yahoo [2], and Baidu [3] internet searches, Twitter posts [4], Wikipedia article views [5], clinicians’ queries [6], and crowd sourced self-reporting mobile apps such as Influenzanet [27] and Flu Near You [28], to track influenza activity. Among them, GFT has received most attention, and has inspired subsequent digital disease detection systems [3, 8, 29, 30, 31, 32]. Interestingly, Google has never made their independent variables public, thus, making it impossible to reproduce and improve the exact methodology behind GFT.

We highlight three limitations of the original GFT algorithm, previously identified in [16, 17]. First, it was shown that a static approach, one that does not take advantage of newly available CDC’s ILI activity reports as the flu season evolves, produced model drift, leading to inaccurate estimates. Second, the idea of aggregating the multiple query terms (the independent variables in the GFT model) into a single variables did not allow for changes in people’s internet search behavior over time (and thus changes in query terms’ abilities to track flu) to be appropriately captured by the algorithm behind GFT. Third, GFT was found to ignore the intrinsic time series properties, such as seasonality of the historically observed ILI activity, thus overlooking potentially crucial information that could help produce accurate real time ILI activity level estimates.

Our new method produces robust and highly accurate ILI activity level estimates by addressing the three aforementioned shortcomings of the multiple GFT engines. Furthermore, we provide a theoretical justification for our methodology, which contains as a special case the model developed in [17]. Our new model not only achieves the goal of (a) dynamically incorporating new information from CDC reports as they become available and (b) automatically selecting the most useful Google search queries for estimation as in [17], but it also largely improves estimation by (c) including the long-term cyclic information (seasonality) from past flu seasons on record as input variables, and (d) using a two-year moving window (which immediately precedes the desired date of estimation) for the training period to capture the most recent behavior in people’s search patterns. Even though we use as input only the publicly available, low-quality data acquired from the *Google Correlate* and *Google Trends* websites, our new method has significant improvement over the latest version of GFT.

We name our model ARGO, which stands for AutoRegression with GOogle search data. Statistically speaking, ARGO is an autoregressive model with Google search queries as exogenous variables; ARGO also employs L_1 (and potentially L_2) regularization. The autoregressive part captures the seasonality of historical ILI activity level, while the exogenous part exploits the prediction power of Google search queries. L_1 and L_2 penalties are used to achieve automatic selection of most relevant information. Our framework is easy to generalize to early detection systems aimed at using internet search information to track seasonal social events in public health, business, and others.

Although our framework is capable of generating models that forecast ILI activity weeks into the future, we decided to focus here on real-time ILI activity tracking.

1 Results

Retrospective estimates of influenza activity (ILI activity level, as reported by the CDC) were produced using our model, ARGO, for the time period of March 29, 2009 to April 25, 2015, assuming we had access only to the historical CDC’s ILI activity reports up to the previous week of estimation. We compared ARGO’s estimates with the ground truth: the CDC-reported weighted ILI activity level, published typically with one or two weeks delay, by calculating a collection of accuracy metrics described in the materials section. These metrics include the Root Mean Squared Error (RMSE), the Mean Absolute Error (MAE), Correlation with estimation target, and Correlation of increment with estimation target (Corr. of increment). For comparison, we calculated these accuracy metrics for (a) GFT estimates (accessed on April 25, 2015), (b) estimates produced using the methodologies of Santillana et al. 2014 [6, 17], (c) estimates produced with an AR(3) autoregressive model ([4, 16]), and (d) a naive method that simply uses the value of the prior week’s CDC’s ILI activity level as the estimate for the current one.

Table 1 summarizes these accuracy metrics for all estimation methods for multiple time periods. The first column shows that ARGO’s estimates outperform all other alternatives, in every accuracy metric, for the whole time period. The other columns of Table 1 show the performance of all the methods for the 2009 off-season H1N1 flu outbreak, and each regular flu season since 2010.

	Whole period	Off-season flu	Regular flu seasons (week 40 to week 20 next year)				
		H1N1	2010-11	2011-12	2012-13	2013-14	2014-15 partial
RMSE							
ARGO	0.637	0.655	0.618	0.830	0.679	0.308	0.593
GFT (Oct 2014)	2.213	0.773	1.110	3.023	4.451	0.981	0.683
Santillana et al. (2014)	0.909	0.945	0.864	1.688	0.918	0.495	0.683
AR(3)	0.955	0.813	0.794	1.051	1.191	0.966	0.924
Naive	1.000 (0.354)	1.000 (0.600)	1.000 (0.339)	1.000 (0.163)	1.000 (0.499)	1.000 (0.350)	1.000 (0.500)
MAE							
ARGO	0.680	0.607	0.588	0.760	0.653	0.406	0.673
GFT (Oct 2014)	1.828	0.777	1.260	3.277	5.028	0.884	0.726
Santillana et al. (2014)	1.035	0.793	0.977	1.782	0.897	0.634	0.872
AR(3)	0.920	0.777	0.787	0.951	0.988	0.915	0.924
Naive	1.000 (0.206)	1.000 (0.425)	1.000 (0.259)	1.000 (0.135)	1.000 (0.325)	1.000 (0.213)	1.000 (0.332)
Correlation							
ARGO	0.984	0.984	0.988	0.924	0.968	0.993	0.981
GFT (Oct 2014)	0.874	0.989	0.968	0.833	0.926	0.969	0.984
Santillana et al. (2014)	0.970	0.959	0.982	0.898	0.960	0.982	0.967
AR(3)	0.963	0.968	0.971	0.877	0.903	0.928	0.939
Naive	0.960	0.951	0.954	0.887	0.924	0.923	0.929
Corr. of increment							
ARGO	0.744	0.796	0.793	0.309	0.532	0.944	0.851
GFT (Oct 2014)	0.706	0.863	0.702	0.484	0.502	0.849	0.910
Santillana et al. (2014)	0.671	0.782	0.688	0.599	0.375	0.882	0.738
AR(3)	0.386	0.585	0.569	0.077	0.011	0.414	0.498
Naive	0.438	0.602	0.570	0.095	0.134	0.415	0.518

Table 1: Comparison of different models for the estimation of influenza epidemics. Boldface highlights the best value for each performance metric in each study period. RMSE and MAE are relative to the error of naive method, that is, the number reported is the ratio of error of a given method to that of the naive method. The absolute error of the naive method, which simply uses the prior week’s ILI activity level as the estimate for the following one, is reported in the parentheses.

The panels of Figure 1 graphically present the estimates against the observed CDC-reported ILI activity level. Close inspection shows that, in the post-2009 regular flu seasons, ARGO uniformly outperformed all other alternative estimation methods in terms of both root mean squared error and

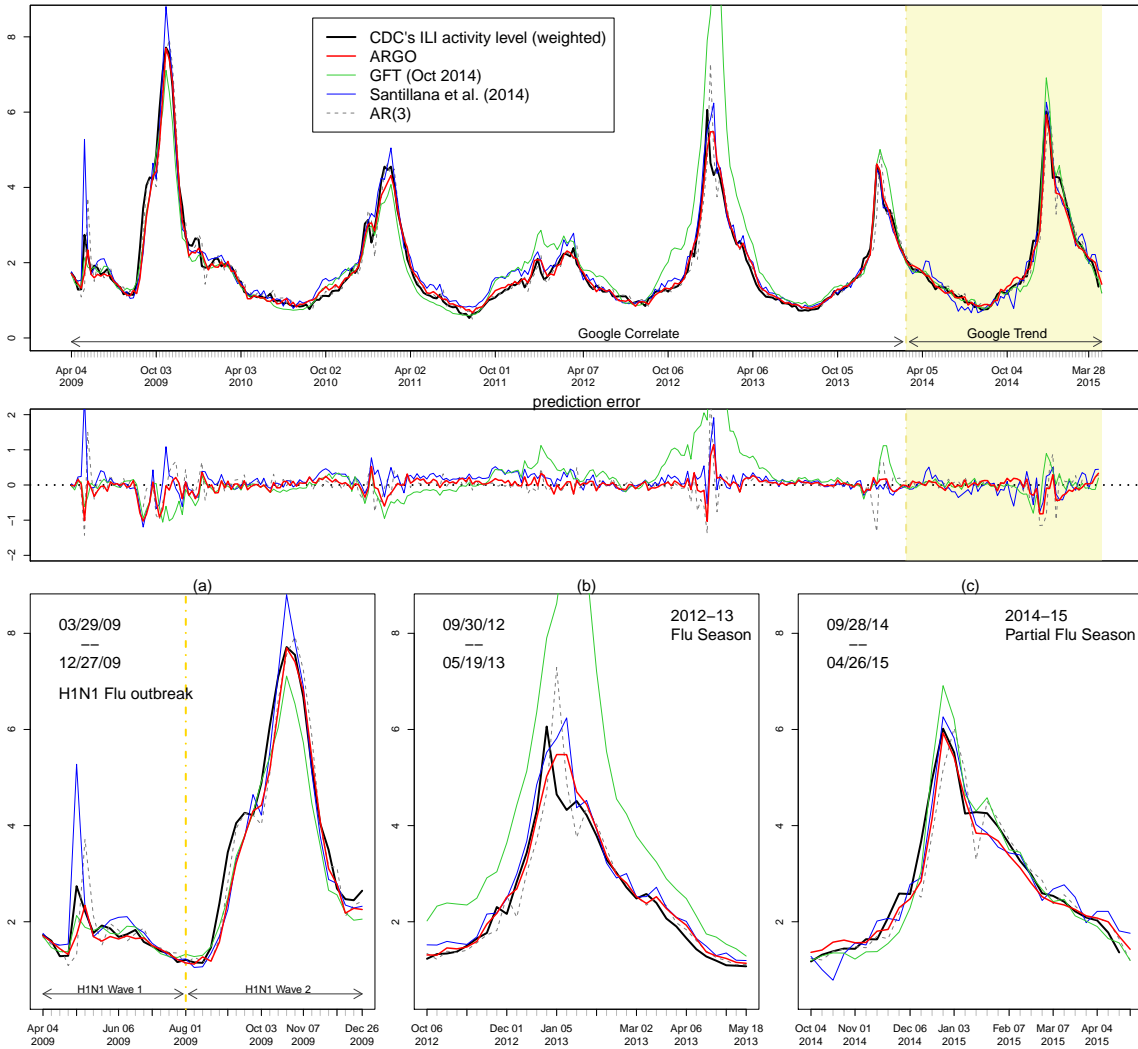


Figure 1: Estimation results. The top panel shows the estimated ILI activity level from ARGO (thick red), contrasting to the true CDC's ILI activity level (thick black) as well as the estimates from GFT (green), method of Santillana et al. [17] (blue) and AR(3) model (dashed grey). The two background shades, white and yellow, reflect two data sources, *Google Correlate* and *Google Trends*, respectively. The second panel shows the estimation error, defined as estimated value minus the CDC's ILI activity level. A positive error suggests over-estimation and a negative error suggests under-estimation. The small panels labeled in alphabetical order are zoomed-in plots for estimation results in different study periods. Panel (a) is the H1N1 flu outbreak period. Panel (b) is the 2012-13 regular flu season (week 40 of year 2012 to week 20 of year 2013). Panel (c) is the 2014-15 regular flu season. At the time of this paper 2014-15 season is still ongoing so only partial season from week 40 of year 2014 to week 16 of year 2015 is studied.

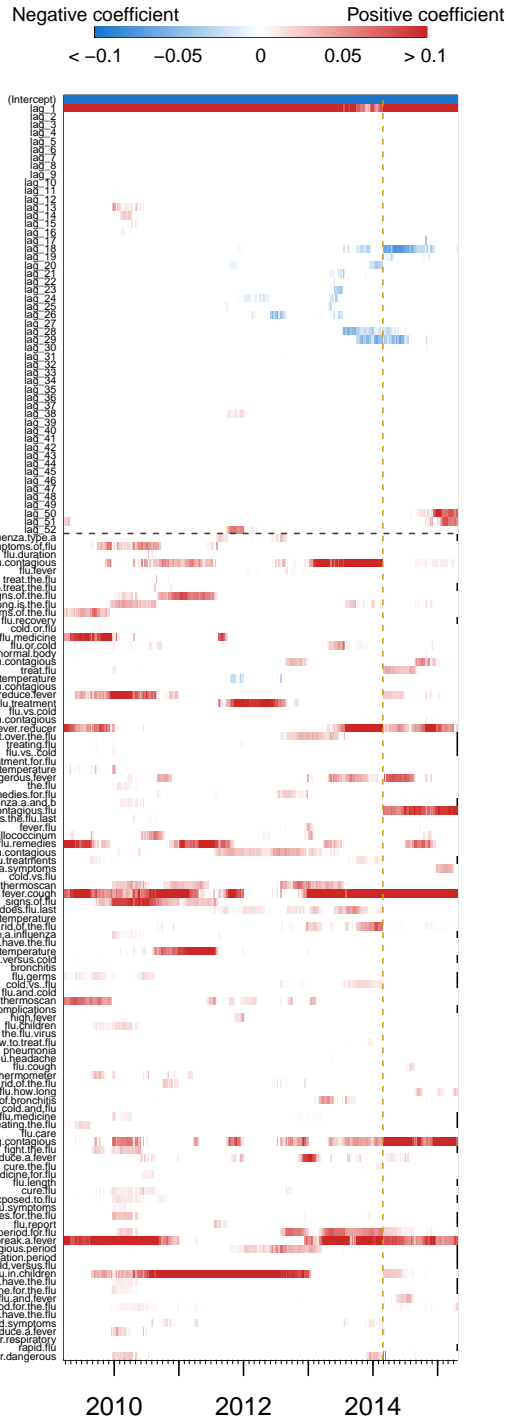


Figure 2: Dynamic coefficients for ARGO. Red color represents positive coefficients, blue color represents negative coefficients, and white color represents zero. Black horizontal dashed line separates Google search queries from autoregressive lags, and yellow vertical dashed line separates coefficients trained on *Google Correlate* data from those trained on *Google Trends* data.

mean absolute error. In terms of correlation, ARGO had higher correlation almost uniformly for all seasons compared to all other alternatives, except for the last season (2014-15 partial season) where ARGO ($r=98.1\%$) had competitive performance to GFT ($r=98.4\%$). ARGO avoids the notorious over-shooting problem of GFT, as seen in Figure 1.

During the 2009 off-season H1N1 flu outbreak, ARGO had the smallest root mean squared error and mean absolute error. In terms of correlation, ARGO ($r=98.4\%$) had similar performance to (the potentially in-sample data of) GFT ($r=98.9\%$) [15], while outperforming all the other alternatives.

It is well-known that CDC reports undergo revisions weeks after their initial publication. These revisions respond to internal consistency checks and in principle lead to more accurate estimates of patients with ILI symptoms seeking medical attention. As a consequence, the available historical CDC information, in a given week, is not necessarily as accurate as it will be. In order to test the effect of using (potentially inaccurate) unrevised information close to the week of estimation, we obtained the historical unrevised and revised reports, as well as the dates when the reports were revised, from the CDC website for the time period of our study. We then used only the information that would have been available to us, at the time of estimation, and produced a time series of estimates for the whole time period described before. We compared our estimates to all other methods and found that ARGO still outperformed all previous methodologies. Moreover, the values of all four accuracy metrics for ARGO essentially did not change, suggesting a desirable robustness to CDC's ILI activity report revision. The results are shown in Table 3 in the appendices.

We faced an additional challenge when producing real-time estimates during the 2014-2015 flu season. The only independent variables available to us at the time of writing this article came from the *Google Trends* website. The information from *Google Trends* has even lower quality than its counterpart from *Google Correlate*, and changes every week as a consequence of constant renormalizations and algorithm updates. These undesired changes affected the quality of our estimates. In order to assess the stability (and thus the quality) of ARGO in the presence of these variations in the data, we obtained the search frequencies of the same query terms (see Figure 2) from *Google Trends* website on 25 different days during the month of April 2015, and produced a set of 25 historical estimates using ARGO. The results of the accuracy metrics associated to these estimates are shown in Table 4 on the appendices. This table shows that, despite the observed variation due to changes in the *Google Trends* input variables, ARGO is threefold more stable than the method of Santillana et al. [17] and still outperforms on average any other method.

2 Discussion

The results presented here demonstrate the superiority of our approach both in terms of accuracy and robustness, when compared to all existing flu tracking models based on Google searches. The value of these results is even higher given the fact that they were produced with low quality input variables. It is highly likely that our methodology would lead to even more accurate results if we were given access to the input variables that Google uses to calculate their estimates.

The incorporation of seasonal flu information appears to be a key factor in the enhanced accuracy of ARGO. The level of ILI activity last week typically has a significant effect on the current level of ILI activity, and ILI activity half a year ago and/or one year ago could provide further information, as shown in Figure 2, which reflects a strong temporal auto-correlation. The integration of time series information leads to a smooth and continuous estimation curve and prevents undesired spikes. Interestingly, once the time series information is included in the model, fewer Google search query terms remain significant, resulting in increased sparsity. For example, among 100 *Google Correlate* query terms, ARGO selected 14 terms on average each week, whereas the method of Santillana et al.

[17] selected 38 terms on average each week. The combination of ARGO’s smoothness and sparsity lead to a substantial reduction on the estimation errors.

Our methodology allows us to transparently understand how Google search information and historical flu information complement one another in different time periods. Time series models tend to be slow in response to sudden observed changes in CDC’s ILI activity level. The naive method, which uses the prior week’s CDC’s ILI activity level as the estimate for the current one, is an extreme case. The AR(3) model shows this “delaying” effect as well, despite its seemingly good correlation and error rate for ILI activity level. Google searches, on the other hand, are better at detecting sudden ILI activity changes, but are also very sensitive to public’s over-reaction to crises.

To investigate further the responsiveness (co-movement) of ARGO towards the change in ILI activity, we calculated the correlation of increment between each estimation model and CDC’s ILI activity level. The correlation of increment between two time series a_t and b_t is defined as $\text{Corr}(a_t - a_{t-1}, b_t - b_{t-1})$, which naturally measures how responsive a_t is to the change in b_t . It is apparent from Table 1 that ARGO has similar responsiveness with GFT and the method of Santillana et al. [17], while outperforming the smoother time series model AR(3) uniformly. The reason behind ARGO’s competitive responsiveness with GFT is evident from Figure 2, where we can see that ARGO globally selects many more Google components than autoregressive components.

A closer look at Figure 2 allows us to see the tendency of time series information (seasonality) to pull ARGO’s estimation towards the historical level. This was evident at the onset of wave 1 of the off-season H1N1 flu outbreak (week ending at 05/02/2009), which resulted in ARGO’s under-estimation. ARGO self-corrected its performance the following week by shifting a portion of model weights from the time series domain to the Google searches domain. Inversely, at the height of 2012-13 season, ARGO, GFT, and method of Santillana et al. [17], all missed the peak due to an apparent unprecedented increase in search activity around this time. ARGO achieved the fastest self-correction by redistributing the weights not only across Google terms but also across time series terms, and thus missed the peak only by 1 week (as opposed to 2 weeks for method of Santillana et al. [17] and about 4 weeks for GFT).

It is important to note that ARGO is robust to potential inaccuracies in the input data, such as CDC’s ILI reports late revisions and variations in the *Google Trends* data due to renormalizations and algorithm updates. This is observed quantitatively in Tables 3 and 4 of the appendices. Moreover, while we have used CDC’s ILI as our gold standard for influenza activity in the US population, our methodology can be immediately adapted to make use of any other measurement of influenza activity that may prove to be more appropriate or accurate in the future.

2.1 Limitations

While ARGO displays a clear superiority over previous methods, it is not fail-proof. Since it relies on the public’s search behavior, any abrupt changes to the inner works of Google’s search engine or any changes in the way health-related search information is displayed to users will affect the accuracy of our methodology [33, 34]. We expect that ARGO will be fast at correcting itself if any changes take place in the future.

2.2 Next steps

ARGO can be easily generalized to any temporal and spatial scales for a variety of diseases or social events amenable to be tracked by Google searches [3, 8, 9, 29, 30, 35, 36]. Moreover, our methodological framework provides a clear strategy to identify optimally performing methods to track social events using information from other internet-based services such as Twitter [4].

3 Data sources

We used the normalized search volume of Google search queries that are most highly correlated with CDC’s Weighted ILI as our independent variables. Google normalizes raw search volume of each query by dividing through the total search volume, so that normalized search volumes from different years are comparable. These data are available at the *Google Correlate* website (<https://www.google.com/trends/correlate>. Date of access: April 25, 2015). *Google Correlate* standardized normalized search volume of each query to have zero mean and one standard deviation across time. We note that the dataset from *Google Correlate* contains data only from 2004 to Feb 2014; thus, in order to obtain the real-time search frequencies after Feb 2014, we manually entered the search query terms in *Google Trends*, (<http://www.google.com/trends>. Date of access: April 25, 2015). *Google Trends* provides even lower quality data (than *Google Correlate*): search volume of each query is given in an integer scale from 0 to 100. To make *Google Correlate* data compatible with *Google Trends* data, we linearly transformed the *Google Correlate* data to the same scale of 0 to 100 in our analysis. We used *Google Correlate* data up to its last available date, and then switched to *Google Trends* data afterwards. This is indicated in Figure 1 by different shades of the background.

Our analyses use the weighted version of CDC’s ILI activity level as the estimation target (available at <http://gis.cdc.gov/grasp/fluview/fluportaldashboard.html>. Date of access: April 25, 2015). The weekly revisions of CDC’s ILI are available at the CDC website for all recorded seasons (from week 40 of a given year to week 20 of the subsequent year). For example, ILI activity report revision at week 50 of season 2012-2013 is available at <http://www.cdc.gov/flu/weekly/weeklyarchives2012-2013/data/senAllregt50.htm>; ILI activity report revision at week 9 of season 2014-2015 is available at <http://www.cdc.gov/flu/weekly/weeklyarchives2014-2015/data/senAllregt09.html> (the webpage has suffix “htm” for seasons before 2014-2015 and suffix “html” for 2014-2015 season).

We used the latest version of Google Flu Trends weekly estimate of current ILI activity level as one of our comparison methods in the analyses. Google updates its Flu Trends algorithm from time to time. The current version (4th version, revised in Oct 2014) of GFT is available at <https://www.google.org/flutrends/us/data.txt> (Date of access: April 25, 2015).

4 Formulation of the model

Our model, ARGO, is motivated by a hidden Markov model. The *logit*-transformed CDC-reported ILI activity level $\{y_t\}$ is the intrinsic time series of interest. We impose a simple autoregressive (AR) model with lag N on it, which implies that the collection of vectors $\{y_{(t-N+1):t}\}_{t \geq N}$ is a Markov chain. The vector of *log*-transformed normalized volume of Google search queries at time t , \mathbf{X}_t , depends only on the ILI activity at the same time, y_t (this follows the intuition that people’s online searches are in response of real flu occurrences). The Markovian property on block $y_{(t-N+1):t}$ leads to the (vector) hidden Markov model structure.

$$\begin{array}{ccccccc}
 y_{1:N} & \rightarrow & y_{2:(N+1)} & \rightarrow & \cdots & \rightarrow & y_{(T-N+1):T} \\
 \downarrow & & \downarrow & & & & \downarrow \\
 \mathbf{X}_N & & \mathbf{X}_{N+1} & & & & \mathbf{X}_T
 \end{array} \tag{1}$$

We assume normality on y_t and \mathbf{X}_t . Therefore our formal mathematical assumptions are:

1. $y_t = \mu_y + \sum_{j=1}^N \alpha_j y_{t-j} + \epsilon_t, \quad \epsilon_t \stackrel{iid}{\sim} \mathcal{N}(0, \sigma^2)$
2. $\mathbf{X}_t | y_t \sim \mathcal{N}_K(\mu_x + y_t \beta, \mathbf{Q})$

3. Conditional on y_t , \mathbf{X}_t is independent of $\{y_l, \mathbf{X}_l : l \neq t\}$

where $\boldsymbol{\beta} = (\beta_1, \beta_2, \dots, \beta_K)^\top$, $\boldsymbol{\mu}_x = (\mu_{x_1}, \mu_{x_2}, \dots, \mu_{x_K})^\top$, and \mathbf{Q} is the covariance matrix.

To make the data more normal, we transform the original ILI activity level from $[0, 1]$ to \mathbb{R} using the logit function, obtaining the y_t , and transform the Google search volumes from $[0, 100]$ to \mathbb{R} using the log function, obtaining the \mathbf{X}_t . The log function is appropriate because Google search frequencies usually have exponential growth rate near peaks and are artificially scaled to $[0, 100]$ by dividing the running maximum. Since *Google Trends* is in integer scale from 0 to 100, we add a small number $\delta = 0.5$ before the transformation to avoid taking the log of 0.

The predictive distribution $p(y_t | y_{1:(t-1)}, \mathbf{X}_{1:t})$ is a normal distribution, whose mean is a linear combination of $y_{(t-N):(t-1)}$ and \mathbf{X}_t , and whose variance is a constant. This observation leads to equation (2) below, which defines the ARGO model. Detailed formulas for the predictive distribution are given in the appendices.

5 The ARGO model

Let y_t be the *logit*-transformed CDC's (weighted) ILI activity level at time t , and $X_{i,t}$ the *log*-transformed Google search frequency of term i at time t . Our ARGO model is given by

$$y_t = \mu_y + \sum_{j=1}^N \alpha_j y_{t-j} + \sum_{i=1}^K \beta_i X_{i,t} + \epsilon_t, \quad \epsilon_t \stackrel{iid}{\sim} \mathcal{N}(0, \sigma^2) \quad (2)$$

where \mathbf{X}_t can be thought as the exogenous variables to time series $\{y_t\}$.

6 Parameter estimation of ARGO model

We chose $N = 52$ (weeks) to capture the within-year seasonality in ILI activity, and $K = 100$ (Google search terms) following the data availability from *Google Correlate*. Since we have more independent variables than the number of observations, the usual maximum likelihood estimate (ordinary least squares) method will fail. Therefore we have to impose regularities for parameter estimation and invoke penalized likelihood. In general we have three kinds of penalties, L_1 penalty [37], L_2 penalty [38], and elastic net penalty, which is a linear combination of L_1 and L_2 penalties [39]. All parameters are dynamically trained every week with a 2-year (104 weeks) rolling window. In a given week t , the goal is to find parameters μ_y , $\boldsymbol{\alpha} = (\alpha_1, \dots, \alpha_{52})$, and $\boldsymbol{\beta} = (\beta_1, \dots, \beta_{100})$, that minimize

$$\sum_t \left(y_t - \mu_y - \sum_{j=1}^{52} \alpha_j y_{t-j} - \sum_{i=1}^{100} \beta_i X_{i,t} \right)^2 + \lambda_\alpha \|\boldsymbol{\alpha}\|_1 + \eta_\alpha \|\boldsymbol{\alpha}\|_2^2 + \lambda_\beta \|\boldsymbol{\beta}\|_1 + \eta_\beta \|\boldsymbol{\beta}\|_2^2 \quad (3)$$

where $\lambda_\alpha, \lambda_\beta, \eta_\alpha, \eta_\beta$ are hyper-parameters.

Values of hyper-parameters have considerable influence on the estimation of $\boldsymbol{\alpha}, \boldsymbol{\beta}$. Should we have infinite amount of data, we could use cross-validation to select all 4 hyper-parameters. However, since we used a two-year moving window to dynamically train our models, we have only 104 training data points at a given week, and as a consequence, the cross-validation result is highly variable. Therefore, we need to pre-specify some of the hyper-parameters to reduce cross-validation noise. For model simplicity and sparsity, combining with the evidence seen from cross-validation, we set

$\eta_\alpha = \eta_\beta = 0$. This lead to an L_1 penalization on both autoregressive terms and Google search queries. With L_1 penalty, ARGO tends to zero out unnecessary α_i, β_i , thus archives variance reduction and variables selection [37]. Still, with the remaining two hyper-parameters λ_α and λ_β , the cross-validation results remain to have considerable variance. By the same sparsity and simplicity argument, we further constrained $\lambda_\alpha = \lambda_\beta$. Therefore, the ARGO model we finally propose is equation (3) but with constraint $\eta_\alpha = \eta_\beta = 0$ and $\lambda_\alpha = \lambda_\beta$. A detailed discussion of our specification of the hyper-parameters is provided in the appendices.

6.1 Accuracy metrics

The Root Mean Squared Error (RMSE) of estimator \hat{y} to target y is defined as

$$\text{RMSE}(\hat{y}_t, y_t) = \sqrt{\frac{1}{n} \sum_{t=1}^n (\hat{y}_t - y_t)^2}.$$

The Mean Absolute Error (MAE) of estimator \hat{y} to target y is defined as

$$\text{MAE}(\hat{y}_t, y_t) = \frac{1}{n} \sum_{t=1}^n |\hat{y}_t - y_t|.$$

The correlation of estimator \hat{y} to target y is their sample correlation coefficient. The correlation of increment between two time series \hat{y}_t, y_t measures the co-movement of estimator and the target. It is defined as

$$\text{Corr. of increment}(\hat{y}_t, y_t) = \text{Corr}(\hat{y}_t - \hat{y}_{t-1}, y_t - y_{t-1})$$

Appendices

Details of our methodology are presented as follows. First, the predictive distribution in the formulation of the ARGO model and the corresponding assumptions are discussed; second, the statistical strategy to determine the hyper-parameters of the ARGO model is explained; third, the results of two sensitivity analysis aimed at testing the robustness of the ARGO methodology, (a) with respect to subsequent revisions of CDC’s ILI activity reports, and (b) with respect to observed variation of the input variables coming from *Google Trends* data, are presented.

A Predictive distribution in the formulation of ARGO model

To improve normality in the distribution of data for both the input variables and the dependent variables, the CDC-reported ILI activity level was *logit*-transformed, and the normalized volume of Google search queries were *log*-transformed. These transformations led to two sets of variables, the intrinsic (influenza epidemics activity) time series of interest $\{y_t\}$, and the (Google search) variable vector \mathbf{X}_t at time t (that depends only on y_t), respectively. Our formal mathematical assumptions are:

1. $y_t = \mu_y + \sum_{j=1}^N \alpha_j y_{t-j} + \epsilon_t, \quad \epsilon_t \stackrel{iid}{\sim} \mathcal{N}(0, \sigma^2)$
2. $\mathbf{X}_t | y_t \sim \mathcal{N}_K(\boldsymbol{\mu}_x + y_t \boldsymbol{\beta}, \mathbf{Q})$
3. Conditional on y_t , \mathbf{X}_t is independent of $\{y_l, \mathbf{X}_l : l \neq t\}$

where $\boldsymbol{\beta} = (\beta_1, \beta_2, \dots, \beta_K)^\top$, $\boldsymbol{\mu}_x = (\mu_{x_1}, \mu_{x_2}, \dots, \mu_{x_K})^\top$, \mathbf{Q} is the covariance matrix. We can calculate the predictive distribution $p\left(y_{t+1} \mid y_{1:t}, \mathbf{X}_{1:(t+1)}\right)$ as

$$\begin{aligned} & p\left(y_{t+1} \mid y_{1:t}, \mathbf{X}_{1:(t+1)}\right) \\ & \sim \mathcal{N}\left(\left(\frac{1}{\sigma^2} + \boldsymbol{\beta}^\top \mathbf{Q}^{-1} \boldsymbol{\beta}\right)^{-1} \left(\frac{\mu_y + \boldsymbol{\alpha}^\top y_{(t-N+1):t}}{\sigma^2} + \boldsymbol{\beta}^\top \mathbf{Q}^{-1} (\mathbf{x}_{t+1} - \boldsymbol{\mu}_x)\right), \right. \\ & \quad \left. \left(\frac{1}{\sigma^2} + \boldsymbol{\beta}^\top \mathbf{Q}^{-1} \boldsymbol{\beta}\right)^{-1}\right) \end{aligned} \quad (4)$$

which is a normal distribution, whose mean is a linear combination of $y_{(t-N):(t-1)}$ and \mathbf{X}_t , and whose variance is a constant.

B Determination of the hyper-parameters for ARGO

The optimized parameters of the ARGO model, μ_y , $\boldsymbol{\alpha} = (\alpha_1, \dots, \alpha_N)$, $\boldsymbol{\beta} = (\beta_1, \dots, \beta_K)$ are given by

$$\begin{aligned} \arg \min_{\mu_y, \boldsymbol{\alpha}, \boldsymbol{\beta}} \quad & \sum_t \left(y_t - \mu_y - \sum_{j=1}^{52} \alpha_j y_{t-j} - \sum_{i=1}^{100} \beta_i X_{i,t} \right)^2 \\ & + \lambda_\alpha \|\boldsymbol{\alpha}\|_1 + \eta_\alpha \|\boldsymbol{\alpha}\|_2^2 + \lambda_\beta \|\boldsymbol{\beta}\|_1 + \eta_\beta \|\boldsymbol{\beta}\|_2^2. \end{aligned} \quad (5)$$

The training period consists of a two-year (104 weeks or data points) rolling window that immediately precedes the desired date of estimation. The hyper-parameters are $\lambda_\alpha, \lambda_\beta, \eta_\alpha, \eta_\beta$. We tested the performance of ARGO with the following specifications of hyper-parameters:

1. Restrict $\eta_\alpha = \eta_\beta = 0$ and $\lambda_\alpha = \lambda_\beta$, cross validate on λ_α . This is our proposed ARGO with the same L_1 penalty for Google search terms and autoregressive lags.
2. Restrict $\eta_\alpha = \eta_\beta = 0$, cross validate on $(\lambda_\alpha, \lambda_\beta)$. This is ARGO with separate L_1 penalties for Google search terms and autoregressive lags.
3. Restrict $\eta_\alpha = \eta_\beta$ and $\lambda_\alpha = \lambda_\beta = 0$, cross validate on η_α . This is ARGO with the same L_2 penalty for Google search terms and autoregressive lags.
4. Restrict $\lambda_\alpha = \lambda_\beta = 0$, cross validate on $(\eta_\alpha, \eta_\beta)$. This is ARGO with separate L_2 penalties for Google search terms and autoregressive lags.
5. Restrict $\lambda_\alpha = \lambda_\beta, \eta_\alpha = \eta_\beta$, cross validate on $(\lambda_\alpha, \eta_\alpha)$. This is ARGO with the same elastic net (both L_1 and L_2) penalty for Google search terms and autoregressive lags.

Table 2 summarizes the in-sample estimation performance for our proposed ARGO, together with other specifications of hyper-parameters. It is apparent from the table that the L_1 penalty generally performs better than L_2 penalty. The L_1 penalty tends to shrink the coefficients of unnecessary independent variables to be exactly zero, and thus eliminates redundant information; on the other hand, the L_2 penalty can only shrink the coefficients to be close to zero. As a result, L_2 penalized coefficients are not as sparse as their L_1 counterparts. Besides, from Table 2, we see that ARGO with separate L_1 penalties (Specification 2) outperforms ARGO with separate L_2 penalties (Specification

	Whole in-sample period 01/07/07-03/29/09	2006-07 partial season 01/07/07-05/20/07	2007-08 season 09/30/07-05/18/08	2008-09 partial season 09/28/08-03/29/09
RMSE				
ARGO w/ same L_1	0.644	0.697	0.602	0.653
ARGO w/ sep. L_1	0.658	0.672	0.637	0.629
ARGO w/ same L_2	1.165	0.817	1.175	1.243
ARGO w/ sep. L_2	1.010	0.740	0.946	1.173
ARGO w/ ElasticNet	0.669	0.757	0.585	0.766
Naive	1.000 (0.316)	1.000 (0.286)	1.000 (0.473)	1.000 (0.304)
MAE				
ARGO w/ same L_1	0.678	0.651	0.584	0.634
ARGO w/ sep. L_1	0.691	0.671	0.621	0.593
ARGO w/ same L_2	1.223	0.836	1.094	1.469
ARGO w/ sep. L_2	1.149	0.753	0.943	1.401
ARGO w/ ElasticNet	0.738	0.718	0.613	0.780
Naive	1.000 (0.206)	1.000 (0.245)	1.000 (0.335)	1.000 (0.226)
Correlation				
ARGO w/ same L_1	0.987	0.977	0.983	0.977
ARGO w/ sep. L_1	0.986	0.980	0.980	0.976
ARGO w/ same L_2	0.969	0.984	0.976	0.955
ARGO w/ sep. L_2	0.979	0.987	0.983	0.967
ARGO w/ ElasticNet	0.987	0.984	0.986	0.975
Naive	0.965	0.949	0.950	0.935
Corr. of increment				
ARGO w/ same L_1	0.779	0.643	0.857	0.646
ARGO w/ sep. L_1	0.708	0.545	0.758	0.697
ARGO w/ same L_2	0.828	0.793	0.864	0.799
ARGO w/ sep. L_2	0.845	0.795	0.881	0.824
ARGO w/ ElasticNet	0.814	0.835	0.852	0.738
Naive	0.623	0.473	0.756	0.322

Table 2: Comparison of different specifications of hyper-parameters for in-sample study period. “ARGO w/ same L_1 ” is ARGO with the same L_1 penalty for Google search terms and autoregressive lags (Specification 1). “ARGO w/ sep. L_1 ” is ARGO with separate L_1 penalties for Google search terms and autoregressive lags (Specification 2). “ARGO w/ same L_2 ” is ARGO with the same L_2 penalty for Google search terms and autoregressive lags (Specification 3). “ARGO w/ sep. L_2 ” is ARGO with separate L_2 penalties for Google search terms and autoregressive lags (Specification 4). “ARGO w/ ElasticNet” is ARGO with the same elastic net penalty for Google search terms and autoregressive lags (Specification 5). The first column is for the entire in-sample study period. The second column is for 2006-07 partial season. 2006-07 full season is not available because data prior to Jan 2007 is used for training. The third column is for 2007-08 full season. The fourth column is for 2008-09 partial season. 2008-09 full season is not available because our out-of-sample study period starts in Apr 2009. RMSE and MAE are relative to the error of naive method. The absolute error of the naive method is reported in the parentheses.

4), in terms of both root mean squared error and mean absolute error. Similarly, ARGO with the same L_1 penalty (Specification 1) outperforms ARGO with the same L_2 penalty (Specification 3), in terms of both root mean squared error and mean absolute error.

The elastic net model, which combines L_1 penalty and L_2 penalty, does not provide any error reduction. In the cross-validation process of setting $(\lambda_\alpha, \eta_\alpha)$ for elastic net model, 70 weeks out of 116 in-sample weeks showed that the smallest cross-validation mean error when restricting $\eta_\alpha = 0$ (i.e. zero L_2 penalty) is within one standard deviation of the global smallest cross-validation mean error, suggesting that restricting L_2 penalty term to be zero (i.e. $\eta_\alpha = 0$) will introduce little bias. Therefore, for the simplicity and sparsity of the model, we drop the L_2 penalty terms and use only L_1 penalty.

Next we want to decide between the remaining two specifications, ARGO with separate L_1 penalties (Specification 2), or ARGO with the same L_1 penalty (Specification 1). One may argue that Google search terms and autoregressive lags are different sources of information and thus should have different L_1 penalties. However, empirical evidence in Table 2 shows that, again, giving extra flexibility to $(\lambda_\alpha, \lambda_\beta)$ does not generate improvement compared to fixing $\lambda_\alpha = \lambda_\beta$. In the cross-validation process of setting $(\lambda_\alpha, \lambda_\beta)$ for separate L_1 penalties, 99 weeks out of 116 in-sample weeks showed that the smallest cross-validation mean error when restricting $\lambda_\alpha = \lambda_\beta$ (i.e. same L_1 penalty) is within one standard deviation of the global smallest cross-validation mean error. This may well be due to the gain from variance reduction when imposing the restriction $\lambda_\alpha = \lambda_\beta$. Based on the same simplicity and sparsity consideration, we finally decided to restrict $\eta_\alpha = \eta_\beta = 0$ and $\lambda_\alpha = \lambda_\beta$ in the setting of hyper-parameters for ARGO.

C Revision of CDC’s ILI activity reports

Within a flu season, CDC reports are constantly revised to improve their accuracy as new information is incorporated. Thus, CDC’s weighted ILI figures displayed in previously published reports may change in subsequent weeks. As a consequence, in a given week the available CDC ILI information from recent weeks may be inaccurate. To test the robustness of ARGO in the presence of these revisions and mimic the real-time tracking in our retrospective predictions, we trained ARGO and all other alternative models based on the following schedule.

Suppose $z_{i,j}$ is the CDC-reported ILI activity level of week i accessed at week j . Since CDC’s ILI activity report is typically delayed for one week, on week j the historical ILI activity level data we have is $\{z_{i,j} : i \leq j - 1\}$. Due to revisions, ILI activity level of week i accessed at different weeks $z_{i,i+1}, z_{i,i+2}, \dots$ may be different but will converge to a finalized value $z_{i,\infty}$ eventually. Hence, to avoid using forward-looking information, in week j , we train all models with the ILI activity level accessed at that week $\{z_{i,j} : i \leq j - 1\}$. In this sense, any future revision beyond week j will not be incorporated in the training at week j . Yet for the accuracy metrics, the estimation target remains the finalized the ILI activity level $(z_{i,\infty}, i = 1, 2, \dots)$.

Table 3 shows the estimation results when using the aforementioned schedule. Note that ARGO still outperforms all other alternative models. Moreover, the absolute values of all four accuracy metrics for ARGO trained this way essentially do not change compared to ARGO trained with finalized ILI activity level in the main text, indicating the robustness of ARGO.

The weekly revisions of CDC’s ILI activity reports are available at CDC website from week 40 of the year to week 20 of the subsequent year for all seasons studied in this article. For example, ILI activity level revisions at week 50 of season 2012-2013 are available at <http://www.cdc.gov/flu/weekly/weeklyarchives2012-2013/data/senAllregt50.htm>; ILI activity report revision at week 9 of season 2014-2015 is available at <http://www.cdc.gov/flu/weekly/weeklyarchives2014-2015/data/senAllregt09.html> (the webpage has suffix “htm” for seasons before 2014-2015 and suffix “html” for 2014-2015 season).

	Whole period	Off-season flu	Regular flu seasons (week 40 to week 20 next year)				
		H1N1	2010-11	2011-12	2012-13	2013-14	2014-15 partial
	[03/29/09] [04/26/15]	[03/29/09] [12/27/09]	[10/03/10] [05/22/11]	[10/02/11] [05/20/12]	[09/30/12] [05/19/13]	[09/29/13] [05/18/14]	[09/28/14] [04/26/15]
RMSE							
ARGO	0.582	0.611	0.530	0.632	0.625	0.269	0.606
GFT (Oct 2014)	2.002	0.702	0.971	1.878	4.387	0.876	0.700
Santillana et al. (2014)	0.833	0.938	0.773	0.993	0.794	0.436	0.721
AR(3)	0.962	0.805	0.986	1.136	1.087	0.946	0.927
Naive	1.000 (0.391)	1.000 (0.661)	1.000 (0.388)	1.000 (0.263)	1.000 (0.506)	1.000 (0.392)	1.000 (0.487)
MAE							
ARGO	0.570	0.560	0.502	0.581	0.617	0.326	0.678
GFT (Oct 2014)	1.463	0.670	1.093	2.026	5.082	0.742	0.751
Santillana et al. (2014)	0.837	0.770	0.883	1.021	0.802	0.534	0.930
AR(3)	0.997	0.808	0.982	1.158	1.094	0.945	0.910
Naive	1.000 (0.258)	1.000 (0.494)	1.000 (0.299)	1.000 (0.218)	1.000 (0.322)	1.000 (0.254)	1.000 (0.321)
Correlation							
ARGO	0.984	0.981	0.988	0.905	0.970	0.993	0.978
GFT (Oct 2014)	0.874	0.989	0.968	0.833	0.926	0.969	0.984
Santillana et al. (2014)	0.969	0.948	0.980	0.888	0.966	0.983	0.966
AR(3)	0.961	0.965	0.955	0.815	0.921	0.919	0.946
Naive	0.956	0.943	0.946	0.828	0.928	0.909	0.937
Corr. of increment							
ARGO	0.742	0.782	0.773	0.256	0.619	0.929	0.820
GFT (Oct 2014)	0.706	0.863	0.702	0.484	0.502	0.849	0.910
Santillana et al. (2014)	0.643	0.701	0.671	0.605	0.447	0.881	0.741
AR(3)	0.418	0.562	0.554	0.067	0.106	0.360	0.535
Naive	0.454	0.552	0.556	0.162	0.247	0.345	0.577

Table 3: Comparison of different models for the estimation of influenza epidemics, with weekly CDC’s ILI activity level that excludes forward-looking information from ILI activity report revision. The estimation target is the finalized CDC’s ILI activity level. RMSE and MAE are relative to the error of naive method. The absolute error of the naive method is reported in the parentheses.

In this retrospective case study, when the revisions of ILI activity level were not available for a particular week during off-season period, the finalized ILI activity level was used instead.

D Variations of Google Trends data

Google Trends historical data constantly changes as a consequence of re-normalizations and algorithm updates. To study the robustness of ARGO to *Google Trends* data revisions, we obtained the search frequencies of the same search query terms (see Figure 2 in main text) from the *Google Trends* website (<http://www.google.com/trends>) on 25 different days in April 2015. We studied the variability of ARGO’s performance when using these 25 different versions of *Google Trends* data as input variables for the common time period Sep 28, 2014 to Mar 29, 2015. We can study 2014-15 partial season only up to March because this is the longest study period covered by all versions of *Google Trends* data.

Despite the inevitable variation to the revision of the low-quality data from *Google Trends*, ARGO still achieves considerable stability compared to the method of Santillana et al. [17] during this time period. Table 4 suggest that ARGO is threefold more robust than the method of Santillana et al. [17]. The incorporation of time series information helps ARGO achieve the stability. As an extreme example, AR(3) model focuses entirely on the time series information and is thus independent of *Google Trends* data revisions. GFT, formulated with the original search variables as inputs, is by construction insensitive to the changes in *Google Trends* data and displays good stability. For this portion of the study, we included the signal from GFT for context only and we treat it as exogenous in our analysis. Based on the results from previous time periods, it is highly likely that if we had access to Google’s internal raw data (i.e., historical search volume for disease-related phrases) we would have achieved the same stability as well. Yet even with this low-quality data, ARGO outperforms GFT uniformly on all versions of data in terms of both root mean squared error and mean absolute error.

	RMSE	MAE	Correlation	Corr. of increment
Mean				
ARGO	0.223	0.300	0.981	0.838
GFT (Oct 2014)	0.258	0.363	0.985	0.917
Santillana et al. (2014)	0.304	0.392	0.973	0.803
AR(3)	0.333	0.492	0.936	0.487
Standard Deviation				
ARGO	0.014	0.015	0.002	0.012
GFT (Oct 2014)	0.000	0.000	0.000	0.000
Santillana et al. (2014)	0.029	0.042	0.005	0.070
AR(3)	0.000	0.000	0.000	0.000

Table 4: Mean and Standard Deviation of accuracy metrics when using *Google Trends* data accessed at different dates. The common study period is 2014-15 partial season (Sep 28, 2014 to Mar 29, 2015).

References

- [1] Ginsberg J et al. (2009) Detecting influenza epidemics using search engine query data. *Nature* 457:1012–1014. doi:10.1038/nature07634.

- [2] Polgreen PM, Chen Y, Pennock DM, Nelson FD, Weinstein RA (2008) Using internet searches for influenza surveillance. *Clinical Infectious Diseases* 47(11):1443–1448.
- [3] Yuan Q et al. (2013) Monitoring influenza epidemics in China with search query from baidu. *PLoS One* 8(5):e64323.
- [4] Paul MJ, Dredze M, Broniatowski D (2014) Twitter improves influenza forecasting. *PLOS Currents Outbreaks*.
- [5] McIver DJ, Brownstein JS (2014) Wikipedia usage estimates prevalence of influenza-like illness in the United States in near real-time. *PLoS Computational Biology* 10(4):e1003581.
- [6] Santillana M, Nsoesie EO, Mekaru SR, Scales D, Brownstein JS (2014) Using clinicians’ search query data to monitor influenza epidemics. *Clinical Infectious Diseases* 59(10):1446–1450.
- [7] Wesolowski A et al. (2014) Commentary: Containing the Ebola outbreak—the potential and challenge of mobile network data. *PLOS Currents Outbreaks*.
- [8] Chan EH, Sahai V, Conrad C, Brownstein JS (2011) Using web search query data to monitor dengue epidemics: a new model for neglected tropical disease surveillance. *PLoS Neglected Tropical Diseases* 5(5):e1206.
- [9] Preis T, Moat HS, Stanley HE (2013) Quantifying trading behavior in financial markets using google trends. *Scientific Reports* 3(1684).
- [10] Bollen J, Mao H, Zeng X (2011) Twitter mood predicts the stock market. *Journal of Computational Science* 2(1):1–8.
- [11] Wu L, Brynjolfsson E (2015) *The future of prediction: How Google searches foreshadow housing prices and sales*. in *Economic Analysis of the Digital Economy*, eds. Avi Goldfarb SG, Tucker C. (University of Chicago Press), pp. 89–118.
- [12] Bennett J, Lanning S (2007) *The netflix prize*. in *Proceedings of KDD Cup and Workshop 2007*.
- [13] Helft M (2008) Google uses searches to track flu’s spread (The New York Times).
- [14] Butler D (2013) When google got flu wrong. *Nature* 494(7436):155.
- [15] Cook S, Conrad C, Fowlkes AL, Mohebbi MH (2011) Assessing google flu trends performance in the United States during the 2009 influenza virus a (H1N1) pandemic. *PLoS One* 6(8):e23610.
- [16] Lazer D, Kennedy R, King G, Vespignani A (2014) The parable of google flu: Traps in big data analysis. *Science* 343(6176):1203–1205.
- [17] Santillana M, Zhang DW, Althouse BM, Ayers JW (2014) What can digital disease detection learn from (an external revision to) google flu trends? *American Journal of Preventive Medicine* 47(3):341–347.
- [18] Copeland P et al. (2013) Google disease trends: an update. Menlo Park CA: Google.org.
- [19] Stefansen C (2014) Google flu trends gets a brand new engine. <http://googleresearch.blogspot.com/2014/10/google-flu-trends-gets-brand-new-engine.html>.
- [20] WHO (2014) Influenza (seasonal), fact sheet number 211. Accessed April, 2015.

- [21] Shaman J, Karspeck A (2012) Forecasting seasonal outbreaks of influenza. *Proceedings of the National Academy of Sciences* 109(50):20425–20430.
- [22] Chretien JP, George D, Shaman J, Chitale RA, McKenzie FE (2014) Influenza forecasting in human populations: A scoping review. *PloS One* 9(4):e94130.
- [23] Nsoesie E, Mararthe M, Brownstein J (2013) Forecasting peaks of seasonal influenza epidemics. *PLoS Currents* 5.
- [24] Soebiyanto RP, Adimi F, Kiang RK (2010) Modeling and predicting seasonal influenza transmission in warm regions using climatological parameters. *PloS One* 5(3):e9450.
- [25] Shaman J, Karspeck A, Yang W, Tamerius J, Lipsitch M (2013) Real-time influenza forecasts during the 2012–2013 season. *Nature Communications* 4(2837).
- [26] Yang W, Lipsitch M, Shaman J (2015) Inference of seasonal and pandemic influenza transmission dynamics. *Proceedings of the National Academy of Sciences* 112(9):2723–2728.
- [27] Paolotti D et al. (2014) Web-based participatory surveillance of infectious diseases: the influenzanet participatory surveillance experience. *Clinical Microbiology and Infection* 20(1):17–21.
- [28] Smolinski MS et al. (2015) Flu near you: Crowdsourced symptom reporting spanning two influenza seasons. *American Journal of Public Health* .In press.
- [29] Althouse BM, Ng YY, Cummings DA (2011) Prediction of dengue incidence using search query surveillance. *PLoS Neglected Tropical Diseases* 5(8):e1258.
- [30] Ocampo AJ, Chunara R, Brownstein JS (2013) Using search queries for malaria surveillance, Thailand. *Malaria Journal* 12(1):390.
- [31] Scarpino SV, Dimitrov NB, Meyers LA (2012) Optimizing provider recruitment for influenza surveillance networks. *PLoS Computational Biology* 8(4):e1002472.
- [32] Davidson MW, Haim DA, Radin JM (2015) Using networks to combine “big data” and traditional surveillance to improve influenza predictions. *Scientific Reports* 5.
- [33] Tsukayama H (2014) Google is testing live-video medical advice (The Washington Post). Accessed on April 20, 2015.
- [34] Gianatasio D (2014) How this agency cleverly stopped people from googling their medical symptoms: The right ads at the right time (Adweek, Online). Accessed on April 20, 2015.
- [35] Yang AC, Tsai SJ, Huang NE, Peng CK (2011) Association of internet search trends with suicide death in Taipei City, Taiwan, 2004–2009. *Journal of Affective Disorders* 132(1):179–184.
- [36] Cavazos-Rehg PA et al. (2014) Monitoring of non-cigarette tobacco use using google trends. *Tobacco Control*.
- [37] Tibshirani R (1996) Regression shrinkage and selection via the lasso. *Journal of the Royal Statistical Society. Series B (Methodological)* 58(1):267–288.
- [38] Hoerl AE, Kennard RW (1970) Ridge regression: Biased estimation for nonorthogonal problems. *Technometrics* 12(1):55–67.
- [39] Zou H, Hastie T (2005) Regularization and variable selection via the elastic net. *Journal of the Royal Statistical Society: Series B (Statistical Methodology)* 67(2):301–320.